

Synthesis of macroporous β -tricalcium phosphate with controlled porous architectural

M. Descamps^{a,*}, O. Richart^a, P. Hardouin^b, J.C. Hornez^a, A. Leriche^a

^a *Laboratoire des Matériaux et Procédés (LMP), Université de Valenciennes et du Hainaut-Cambrésis, EA 2443, ZI du champ de l'Abbesse, 59600 Maubeuge, France*

^b *Laboratoire de Recherche sur les Biomatériaux et les Biotechnologies (LR2B), Université du Littoral et Côte d'Opale, UPRES EA 2603, BP 120, Quai Masset, 62327 Boulogne sur mer Cedex, France*

Received 31 October 2006; received in revised form 11 December 2006; accepted 30 January 2007

Available online 6 March 2007

Abstract

β -Tricalcium phosphate (TCP) macroporous ceramics were produced by a new manufacturing procedure. A polymeric scaffold constituted of polymethylmethacrylate balls (PMMA), welded together by a thermal forming treatment, is impregnated with a TCP aqueous suspension. After drying step, the thermal removal of the organic compound generates an interconnected macroporosity inside the piece. The coalescence of PMMA balls during the thermal forming treatment follows a sintering mechanism of viscous flow type. This behaviour allows to control the dimension of bridging between particles and thus, the interconnection between pores of sintered material. This new process allows to carry out materials with macropore dimensions which can vary between 100 μm at several millimetres and a perfectly controlled size of interconnection ranging between 0.3 and 0.6 times the macropore diameter. Total porosity volume evolves in an interval from 70 to 80%.

© 2007 Elsevier Ltd and Techna Group S.r.l. All rights reserved.

Keywords: A. Shaping; A. Slip casting; B. Porosity; E. Biomedical applications; β -Tricalcium phosphate

1. Introduction

Porous calcium phosphate ceramics are widely, over the two last decades, used in the clinical field and particularly for the repair and reconstruction of diseased or damaged parts of human body [1–4]. Today, the most used materials are hydroxyapatite and β -tricalcium phosphate. These biomaterials can be colonised by bone tissue, under osteogenic conditions, because of their close resemblance in chemical composition to human bone, their high biocompatibility with surrounding living tissue and their osteoconduction characteristics [5–8]. Moreover, biodegradability of β -tricalcium phosphate allows to consider it as an ideal material for bone reconstruction that should degrade by advancing bone growth [9,10]. However, in order to induce bone ingrowth into porous bioceramic, it is necessary to control the physical characteristics of the implant porosity. Many authors are studied the relationship between

bone ingrowth and pore parameters and in particularly pore size and interconnection size. Results of these works are very various with a macropore size which can vary in the range of 100–1000 μm and a minimal interconnection size of about 20 μm [11–16].

Many processing routes have been utilised for manufacturing macroporous materials. The most used in the literature concern: (1) replicas of porous structures (polymeric sponge) [16–19], (2) addition in the powder or the suspension of porogen organic agents (polyvinylbutyl, polymethylmethacrylate, naphthalene, etc.) [20,21], and (3) introduction of foaming agents into the ceramic slurry (H_2O_2 , etc.) [22–26]. However, limits of these processes are well identified and include for example a partial reproducing and homogeneity of the porous architecture, an uncontrolled size and shape of macropores and interconnection between macropores, low mechanical properties.

Based on these observations, a new manufacturing procedure has been developed to create a material with a fully controlled macroporosity, in terms of shape and size of pores and their interconnections.

* Corresponding author.

E-mail address: michel.descamps@univ-valenciennes.fr (M. Descamps).

2. Experimental procedure

The concept used to perform macroporous ceramics is based on impregnation, with an aqueous calcium phosphate suspension (β -TCP), into a polymeric frame constituted of polymethylmethacrylate balls (PMMA). During the debinding, the thermal removal of these balls (porogen) will generate the macroporosity of material and an interconnection between the macropores whose dimension will depend on the amplitude of bridging between balls. The ceramic skeleton is then sintered to reach a sufficient consolidation.

2.1. Manufacturing of organic frame

The bridging between polymeric balls is obtained by thermal binding. This thermal treatment, allows to carry out a welding to contact points between particles. The temperature choice, and the dwelling time of the treatment allow to control the ball interconnection diameter.

2.1.1. Porogen choice

The PMMA was selected to construct the polymeric frame (DiakonTM Ineos Acrylics Holland). This completely amorphous structure polymer presents the advantages of a thermoplastic behaviour and an easy and clean thermal elimination. Moreover, the spherical shape of this agent allows the building of a frame with close and numerous contacts between particles and a control of the dimension, the morphology and the homogeneity of this compound. Thermal forming trials were carried out on various ball size obtained by mechanical sieving and in particular for diameters in the range of 300–400, 400–500 and 500–600 μm .

2.1.2. Thermal forming process

This operation is carried out at a temperature higher than polymer glass transition point (110 $^{\circ}\text{C}$) in order to allow a viscous flow of matter and thus the formation of necks between

PMMA particles. In order to limit the thermal forming time, and to avoid the organic species deterioration, an intermediate temperature of 180 $^{\circ}\text{C}$ was selected. PMMA balls are introduced into a preheated cylindrical metal mould. The mould diameter is equal to 30 mm and the weight of balls equalises at 6 g. After a thermal forming time, varying 0.5–16 h, the cooling of the organic frame is carried out by a quenching water. The diameter evolution of bridging between the PMMA particles is then evaluated according to the time of thermal forming treatment. This analysis is carried out by scanning electron microscope (Hitachi S-3500N), on the fracture facies of organic particles. Fig. 1 shows this evolution for balls with a ranging between 500 and 600 μm according to thermal forming time.

2.2. Impregnation of the organic frame

The as-prepared organic frame is then impregnated by the calcium phosphate suspension in order to fill the interstitial porosity between the balls. This step required the β -TCP powder synthesis, the slurry optimisation and finally the impregnation of the organic frame by this suspension.

2.2.1. Synthesis and characterisation of β -TCP powder

Stoichiometric β -TCP powder was prepared by aqueous precipitation technique using a diammonium phosphate solution $(\text{NH}_4)_2\text{HPO}_4$ (Carlo Erba, France) and a calcium nitrate solution $\text{Ca}(\text{NO}_3)_2 \cdot 4\text{H}_2\text{O}$ (Brenntag, France).

The solution pH was adjusted at a constant value of 6.5 by a continuous addition of ammonium hydroxide. Temperature was fixed to 30 $^{\circ}\text{C}$ and the solution was matured 24 h. After ripening, solution was filtered and the precipitate was dried to 80 $^{\circ}\text{C}$. Powders obtained with this synthesis process exhibit a too high specific surface area ($>60 \text{ m}^2/\text{g}$) to be easily used for slip casting process. After calcination at 900 $^{\circ}\text{C}$, powder was ground to break up agglomerates formed during the calcination. This grinding step was carried out by ball milling

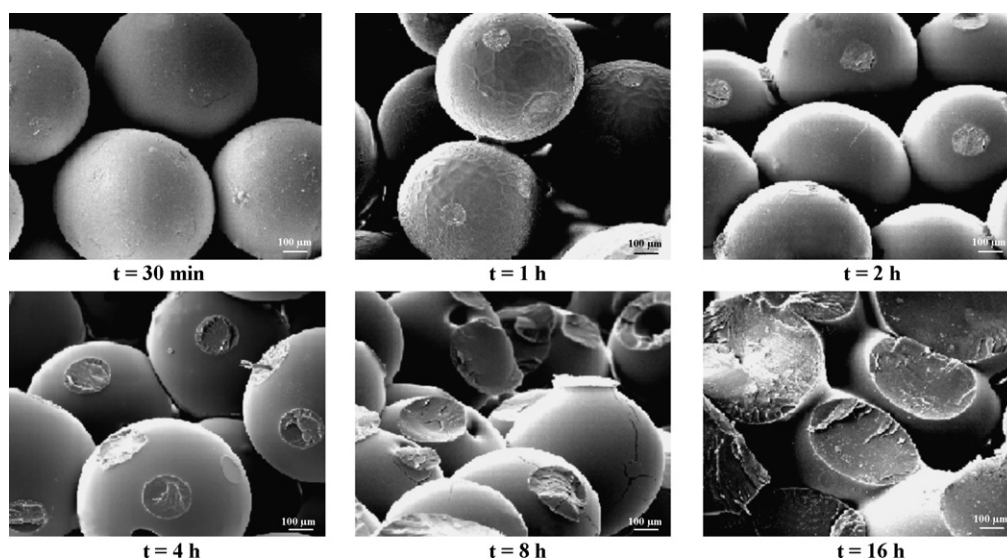


Fig. 1. Fracture facies of the organic frame for balls with a ranging between 500 and 600 μm and thermal formed to 180 $^{\circ}\text{C}$.

with HDPE milling jar and YZT grinding during 3 h. After this treatment, specific surface area of ground powders, recorded by the BET method (Micromeritics, Flow Sorb 3), was equal to $5.2 \text{ m}^2/\text{g}$.

2.2.2. Slip preparation and manufacturing ceramics

β -TCP slurries with a fixed powder concentration of 65 wt.% were prepared in a suspending liquid such as water. In order to enhance slip stability, a commercial organic defloculant (Darvan C, R.t. Vanderbilt Co.) was introduced in amount 1.5 wt.% of β -TCP content. A quantity of binder (Duramax B1001, Rohm and Haas) equal to 4 wt.% of TCP content was added to ensure a consolidation of green material and to avoid the deterioration of material, during the debinding treatment. After a planetary milling during 1 h using agate grinding container and balls, the slip was poured into plaster mould containing the polymeric frame. After drying and demoulding a composite material (PMMA/TCP) is obtained (Fig. 2).

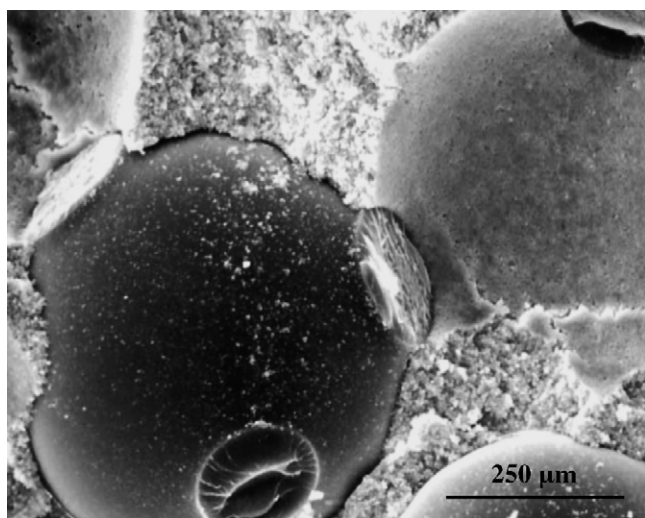


Fig. 2. Organic frame impregnated with β -TCP slurry.

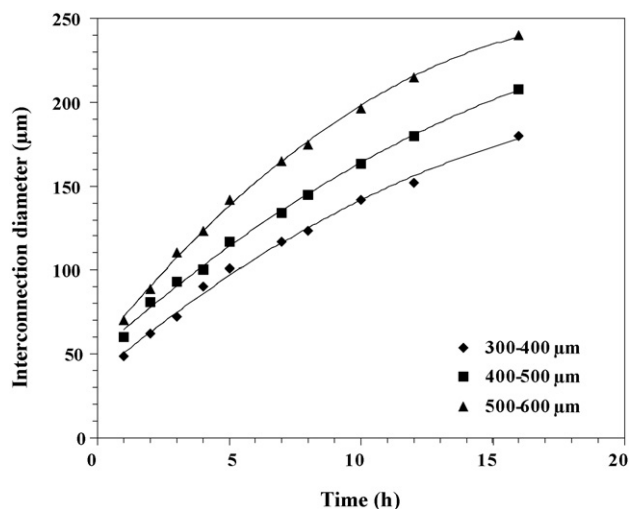


Fig. 3. Evolution of ball interconnection diameters with thermal forming time.

2.3. Thermal treatments

After drying step, the material is debinded to eliminate the PMMA and to generate the macroporosity, then sintered in order to consolidate the ceramic walls. Significant difficulties appeared during the thermal elimination of the polymer. Indeed, the porogen agent occupies a high volume in material, about 70%. So, its degradation produces intense and brutal gaseous emissions and a significant differential expansion between polymer and the ceramic matrix. These phenomena generate internal stresses so high as to lead to the destruction of the ceramic skeleton. Tests carried out with a continuous rise of the temperature with a weak rate of $0.1 \text{ }^\circ\text{C}/\text{min}$ until $400 \text{ }^\circ\text{C}$ led to the deterioration of the product. To avoid this behaviour, the thermal cycle of debinding is optimised and a binder agent is introduced into the suspension of casting.

3. Results and discussion

3.1. Thermal forming of PMMA balls

The sintering of PMMA spherical particles is evaluated by measuring the radius of the contact circle as function of time. Sintering trials performed on various diameters of balls are shown in Fig. 3.

The neck size between particles increases significantly with the processing time. In need, amorphous polymer particles contacting each other at a temperature above the glass transition tend to decrease their total surface area by coalescence. Surface tension is the main driving force playing role in the sintering process.

The theoretical model describing this viscous sintering of two spherical particles in contact was formulated by Frenkel [27] in the case of glassy phases. The matter diffuses from compressive zones (contact surfaces of PMMA balls) to tension zones (particles necks). The neck radius (X) increases with

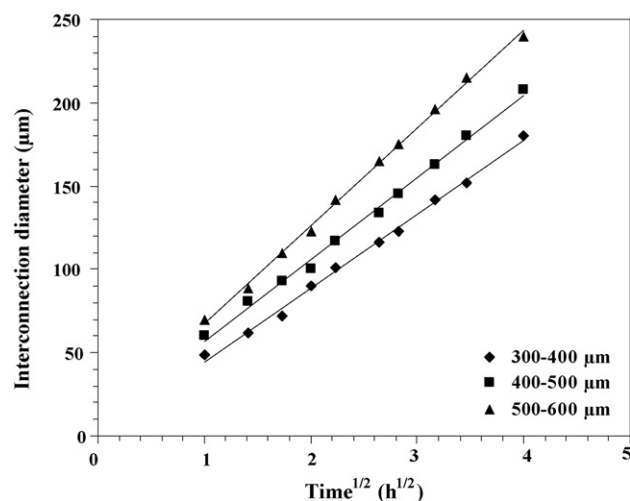


Fig. 4. Evolution of ball interconnection radius with root square of thermal forming time.

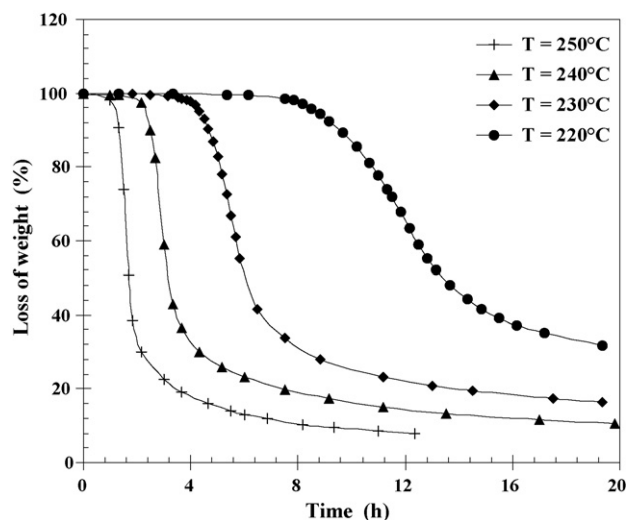


Fig. 5. Isothermal treatments of PMMA at different temperatures.

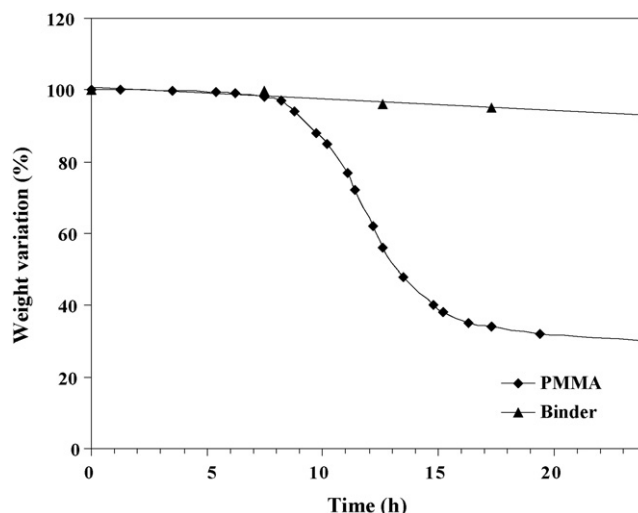


Fig. 7. Weight evolution of binder and PMMA during an isothermal treatment at 220 °C.

thermal treatment duration according to the relation (1):

$$X = \left(\frac{3r\delta t}{2\eta} \right)^{1/2} \quad (1)$$

With δ , η respectively the surface tension and Newtonian viscosity of polymer at considered temperature and r , the PMMA ball radius.

The linear evolution between the neck size of spheres and the square root of the thermal forming time allowed to check the exactitude of the sintering model, which is in agreement with a viscous matter flow between particles (Fig. 4).

3.2. Debinding treatment

PMMA thermogravimetric analysis with heating rate of 0.1 °C/min, indicates a brutal degradation of polymer starting from 220 °C. In order to minimise and to spread out in time the

gaseous emissions resulting from the polymer calcination and thus to reduce stresses within material, this weight loss is analysed during isothermal treatments at temperatures of 220, 230, 240 and 250 °C (Fig. 5). Organic removal velocity strongly decreases when the temperature of treatment diminishes (Fig. 6). At 220 °C this speed is 10 times weaker than at 250 °C and the PMMA weight loss is about 70% after 20 h of treatment. However, the optimisation of the thermal cycle is not enough to obtain samples free from defects after the debinding treatment. So, an organic binder is added to the suspension in order to ensure after drying, a sufficient cohesion between ceramic grains to resist to constraints generated by the PMMA thermal extraction. An acrylic resin aqueous emulsion was chosen because of its high molecular weight, its low viscosity, its low thermal debinding residues level and a very weak degradation thermal at 220 °C, compared to the PMMA (Fig. 7). Various tests allowed to evaluate the sufficient quantity of binder to avoid the deterioration of material, i.e. 4 wt.%

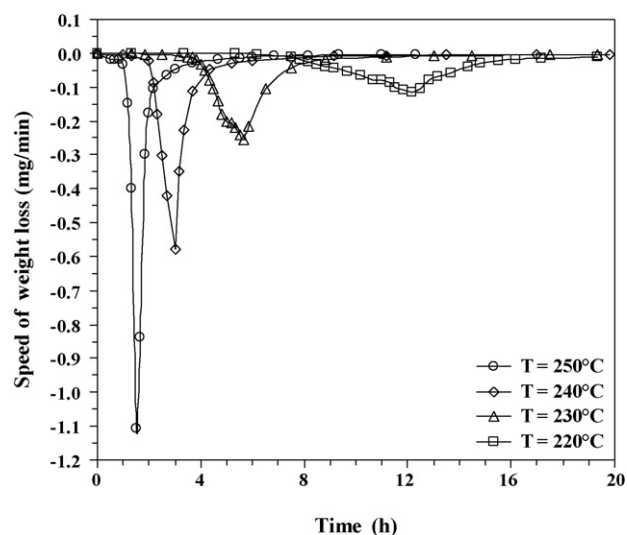


Fig. 6. Removal rate of the PMMA during isothermal treatments carried out at various temperatures.

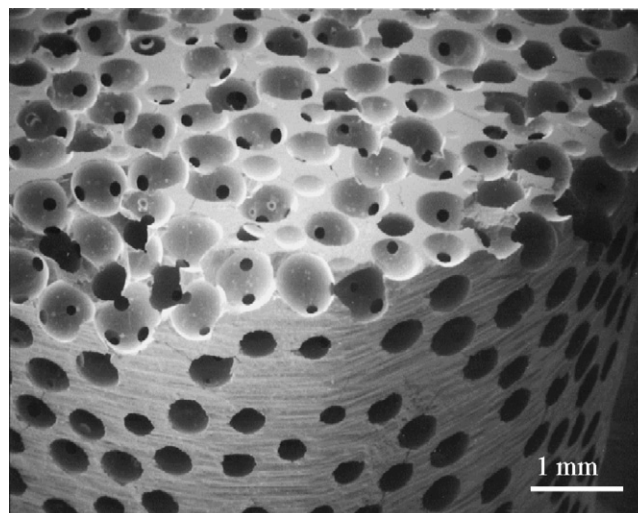


Fig. 8. Typical structure of the macroporous ceramic.

based on the weight of β -TCP. This study made it possible to specify the thermal cycle for the product debinding:

- Heating and cooling rates of 0.1 °C/min.
- Dwell at 220 °C during 30 h in order to eliminate a significant part of the PMMA (70 wt.%).
- Dwell at 400 °C in order to eliminate the totality of organic compounds (residual binder and PMMA, dispersing agent).

3.3. Macroporous parts characterisations

After sintering, the porous characteristics of material are evaluated. Fig. 8 shows a typical structure of the ceramics obtained by this process. This micrograph reveals a spherical macroporosity uniformly distributed in the part with numerous interconnections between the pores. The ceramics walls limiting the pores are smooth and present neither defects or angular parts which could be harmful for the mechanical properties of material (Fig. 9). A preliminary study on the ceramics mechanical properties with a pore diameter material in the range of 400–500 μm showed compressive strength values varying from 16 to 1 MPa for interconnection sizes varying from 80 to 250 μm , respectively. Compressive strength were performed in using an Adamel Lhomargy model DY30 with a 1 kN load cell and a cross-head speed of 0.5 mm min⁻¹. Samples were cylindrical with a diameter $\varnothing = 10$ mm and height $h = 20$ mm.

This elaboration process of macroporous ceramics allows to control many architectural parameters:

- The macropore size which will be related directly to the PMMA ball diameters, by taking into account the shrinkage during the sintering of material. Complementary tests, carried out with varied balls dimensions made it possible to elaborate macroporous parts with a macropore dimension ranging between 100 μm and 1 mm diameter. Fig. 10 illustrates the result obtained with rang balls between 200 and 300 and 600 and 700 μm .
- The interconnection dimension between ceramic macropores is easily controlled by the heating treatment duration. This size can vary between 0.2 and 0.6 times the diameter of the

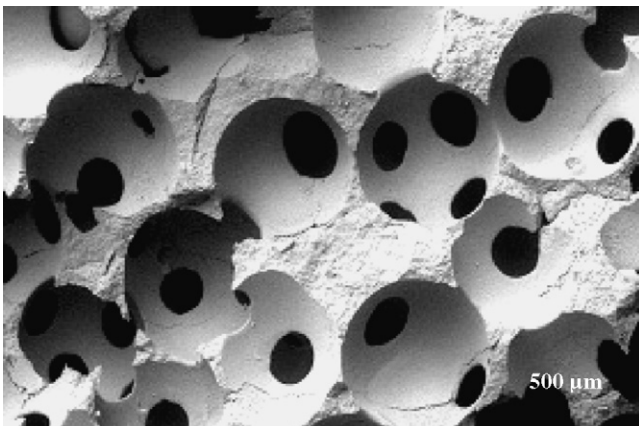
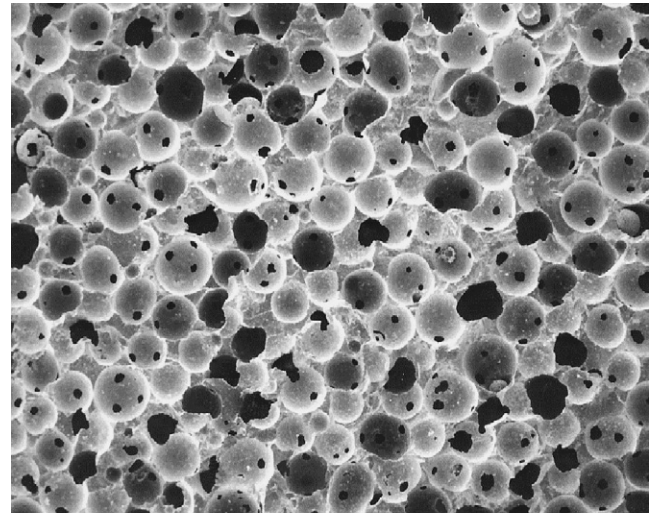
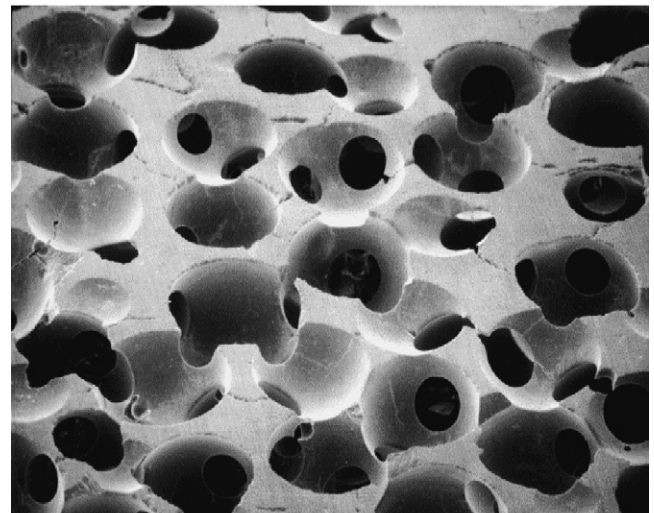


Fig. 9. Aspect of the internal walls of macropores.



Φ pore: 200-300 μm



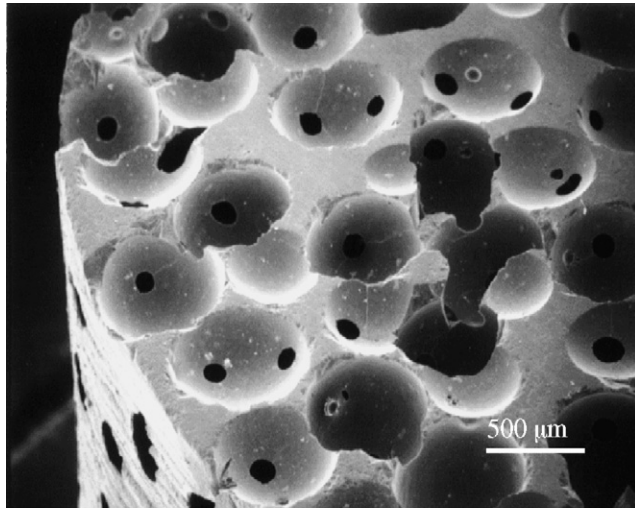
Φ pore: 600-700 μm

Fig. 10. Ceramics with various pore sizes.

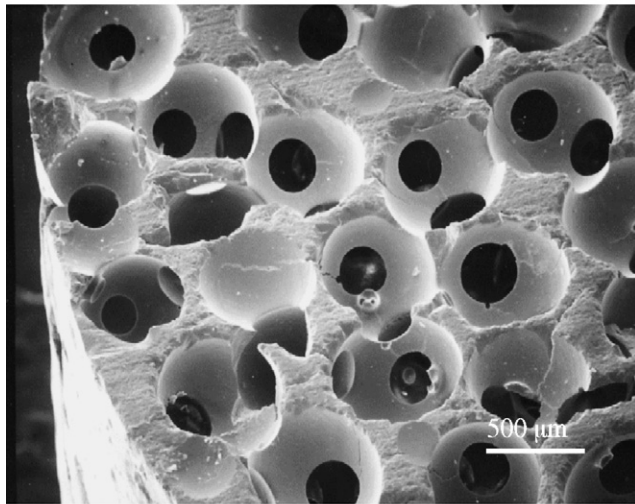
balls, with a precision of about 10%. Fig. 11 shows the evolution of this interconnection for balls of 600–700 μm for various thermal forming times. In this example, dimensions vary from 100 to 260 μm for respectively 2 and 16 h of treatment.

- The porous volume of ceramics can vary between 70 and 80% according to thermal forming time. Indeed, the formation and the growing of the necks are accompanied by a bringing together of the centers of the organic spheres and consequently by a shrinkage of the organic frame. The reduction of interstitial spaces between porogen particles will induce an increase in the porous volume of sintered material.

The pore sizes has been observed as an important factor on bone ingrowth. Many studies carried out on materials with various chemical natures (polymer, metal, ceramic), reveal an important osseous growth when the pore size is higher than 100–150 μm [28,29]. The speed of osseous growth increases with the diameter of the pore, however the quantity of new bone



Φ interconnection : 100 μm



Φ interconnection : 260 μm

Fig. 11. Evolution of the interconnection diameter for various times of thermal forming treatment.

decreases when the section of the pore is too important [30]. For the interconnection sizes between pores, the results obtained are very varied and depend in particular of resorption rate of material. The minimal diameter of interconnection was located at 20 μm for a biodegradable material (β -TCP) [12]. Thus, the control of the porous characteristics of the bone substitute obtained by the thermal forming process makes it possible to adapt the porous structure of the implant according to the type of material used and of the clinical application concerned in order to obtain an optimal efficacy of the biomaterial.

4. Conclusion

This new process for bioceramic realisation allows the control of the various architectural parameters such as, the morphology and size of the porosity and the interconnection size between the macropores which condition the biological effectiveness of biomaterial.

Physical characterisations of these products show that the porous volume of bioceramic can vary from 70 to 80% and the interconnection dimension from 0.2 to 0.6 times the average diameter of the macropore.

Mechanical properties of these materials, in evaluation, and in particular the compressive strength presents significant values, so, this resistance reaches values of about 14 MPa for a material having a porous volume equal to 72%, and macropore and interconnection sizes respectively equal to 400–500 and 100 μm .

This new technology authorises to easily adapt the porous architecture of material to the clinical application concerned, to obtain the shapes and dimensions of samples very various such as cube, stick, parallelepiped, sphere, balls, granules, to carry out products finished without mechanical machining (free of pollution), and finally, the realisation of materials with mechanical reinforcement or with porosity gradient.

References

- [1] L. Hench, Bioceramics, J. Am. Ceram. Soc. 81 (1998) 1705–1728.
- [2] K. de Groot, Effect of porosity and physico-chemical properties on the stability, resorption and strength of calcium phosphate ceramics, Ann. NY Acad. Sci. 253 (1998) 227–233.
- [3] K.J.L. Burg, S. Porter, J.F. Kellam, Biomaterial developments for bone tissue engineering, Biomaterials 21 (2000) 2347–2359.
- [4] M. Jarcho, Calcium phosphate ceramics as hard tissue prosthetics, Clin. Orthop. Rel. Res. 157 (1981) 259–278.
- [5] A. Uchida, S.M.L. Nade, E.R. Mac Cartney, W. Ching, The use of ceramics for bone replacement a comparative study of 3 different porous ceramics, J. Bone Joint Surg. 66 (1984) 269–275.
- [6] R.W. Bucholz, A. Carlton, R.E. Holmes, Hydroxyapatite and tricalcium phosphate bone graft substitutes, Orthop. Clin. N. Am. 18 (1987) 323–334.
- [7] W. Cao, L.L. Hench, Bioactive materials, Ceram. Int. 22 (1996) 493–507.
- [8] P. Ducheyne, Q. Qiu, Bioactive ceramics: the effect of surface reactivity on bone formation and bone cell function, Biomaterials 20 (23–24) (1999) 2287–2303.
- [9] J. Lu, M. Descamps, J. Dejou, G. Koubi, P. Hardouin, J. Lemaître, J.P. Proust, The biodegradation mechanism of calcium phosphate biomaterials in bone, J. Biomed. Mater. Res. (Appl. Biomater.) 63 (2002) 408–412.
- [10] J. Lu, A. Gallur, B. Flautre, K. Anselme, M. Descamps, B. Thierry, P. Hardouin, Comparative study of tissue reaction to calcium phosphate ceramics among cancellous, cortical and medullar bone sites in rabbits, J. Biomed. Mater. Res. 42 (1998) 357–367.
- [11] B. Flautre, M. Descamps, C. Delecourt, M. Blary, Hardouin, Porous HA ceramic for bone replacement: role of the pores and interconnections—experimental study in the rabbit, J. Mater. Sci. Mater. Med. 12 (2001) 679–682.
- [12] J. Lu, B. Flautre, K. Anselme, A. Gallur, M. Descamps, B. Thierry, P. Hardouin, Role of the porous interconnections in porous bioceramics on bone recolonization *in vitro* and *in vivo*, J. Mater. Sci. Mater. Med. 10 (1999) 111–120.
- [13] O. Gauthier, J.M. Bouler, E. Aguado, P. Pilet, G. Daculsi, Macroporous biphasic calcium phosphate ceramics: influence of macropore diameter and macroporosity percentage on bone ingrowth, Biomaterials 19 (1–3) (1998) 133–139.
- [14] P.S. Egli, W. Mueller, R.K. Schenk, Porous hydroxyapatite and tricalcium phosphate cylinders with two different macropore size ranges implanted in the cancellous bone of rabbits, Clin. Orthop. 232 (1998) 127–138.

- [15] B.S. Chang, C.K. Lee, K.S. Hong, H.J. Youn, H.S. Ryu, S.S. Chung, K.W. Park, Osteoconduction at porous hydroxyapatite with various pore configuration, *Biomaterials* 21 (2000) 1291–1298.
- [16] G. Daculsi, N. Passuti, Effect of the macroporosity for osseous substitution of phosphate calcium ceramics, *Biomaterials* 11 (1990) 86–87.
- [17] K. Schwartzwalder, A.V. Somers, US Patent 3,090,094 (1963).
- [18] J. Saggio-Woyanski, C.E. Scott, Processing of porous ceramics, *Am. Ceram. Soc. Bull.* 71 (11) (1992) 1675–1682.
- [19] M. Fabbri, G.C. Celotti, A. Ravaglioli, Hydroxyapatite-based porous aggregates: physico-chemical nature, structure, texture and architecture, *Biomaterials* 16 (1995) 225–228.
- [20] D.M. Liu, Fabrication of hydroxyapatite with controlled porosity, *J. Mater. Sci. Mater. Med.* 8 (1997) 227–232.
- [21] G. Daculsi, N. Passuti, S. Martin, C. Deudon, R.Z. Legeros, S. Raher, Macroporous calcium-phosphate ceramic for long-bone surgery in humans and dogs clinical and histological study, *J. Biomed. Mater. Res.* 24 (1990) 379–396.
- [22] C.P.A.T. Klein, K. de Groot, C. Weiqun, L. Yubao, Z. Xingdong, Osseous substance formation in calcium phosphate ceramics in soft tissues, *Biomaterials* 15 (1994) 31–34.
- [23] L. Yubao, C.P.A.T. Klein, L. Xingdong, K. de Groot, Formation of a bone apatite-like layer on the surface of porous HA ceramics, *Biomaterials* 15 (1994) 835–841.
- [24] E. Ryshkewitch, Compression strength of porous sintered alumina and zirconia, *J. Am. Soc.* 36 (1953) 65–68.
- [25] I.H. Arita, D.S. Wilkinson, M.A. Mondragon, V.M. Castano, Chemistry and sintering behaviour of thin hydroxyapatite ceramics with controlled porosity, *Biomaterials* 16 (1995) 403–408.
- [26] B.V. Rejda, J.G. Peelen, K. de Groot, Tri-calcium phosphate as a bone substitute, *J. Bioeng.* 1 (1977) 93–97.
- [27] J. Frenkel, Viscous flow of crystalline bodies under the action of surface tension, *J. Phys.* 9 (1945) 385–391.
- [28] J.M. Hollis, C.M. Flahiff, Factors affecting bone ingrowth, *Encyclopedic Handbook Biomater. Bioeng.* 1 (1995) 799–821.
- [29] H. Kawahara, Biomaterials for Dental Implants, *Encyclopedic Handbook Biomater. Bioeng.* 2 (1995) 1469–1524.
- [30] P. Predecki, J.E. Stephan, B.A. Auslaender, Kinetics of bone growth into cylindrical channels in aluminium oxide and titanium, *J. Biomed. Mater. Res.* 6 (1972) 375–400.